Thermochimica Acta, 214 (1993) 27–31
Elsevier Science Publishers B.V , Amsterdam

OXIDATION BEHAVIOUR OF Si_3N_4-BASED CERAMICS, STUDIED BY THE THERMOGRAVIMETRIC METHOD.

J. Persson, P.-O. Käll and M. Nygren

Department of Inorganic Chemistry, Arrhenius Laboratory, University of Stockholm, S-10691 Stockholm, Sweden.

Abstract

The oxidation curves of three different Si_3N_4-based ceramics are presented. In most cases, the obtained weight gain curves do not follow the parabolic rate law $(\Delta W/A_0)^2 = K_pt + B$. If crystallization occurs in the formed oxide scale during the experiment, the amorphous cross section area, A, through which oxygen most easily diffuses will decrease with time. With a function A(t), which describes the time dependence of the decrease of A, incorporated into the parabolic rate law one obtains a new rate law which reads $\Delta W/A_0 = a*\arctan\sqrt{bt} + c\sqrt{t}$. It is shown that all oxidation curves can be explained within the framework of this rate law in combination with the parabolic rate law.

1. INTRODUCTION

The oxidation curves of Si_3N_4-based ceramic materials have in most cases been interpreted with the parabolic rate law

$$(\Delta W/A_o)^2 = K_p*t + B \qquad (1)$$

where $\Delta W/A_0$ is the weight gain per surface area unit, K_p is the oxidation rate constant and B an empirical additive constant.

The parabolic rate law is derived from Fick's first law under the assumption that the growth of the oxide scale is controlled by diffusion and that the cross section area, A , through which the rate controlling species diffuses, is constant during the experiment. To the extent that the initially formed amorphous scale devitrifies and /or bubbles, containing released N_2, are formed in the scale during the oxidation, A ought to decrease during the experiment. Recent very accurate oxidation studies of Si_3N_4-based ceramics performed at our laboratory have shown that the parabolic rate law behaviour is rather frequently not obeyed over the entire time interval of the experiment (1-3). In many cases a parabolic rate law behaviour is, however, observed after an initial time lapse, t_0.

This paper was presented at the 13th Nordic Symposium on Thermal Analysis and Calorimetry, Stockholm, Sweden, 9–11 June 1992

However, in some cases, no part of the obtained weight gain curves can be fitted to equation 1. We have also observed that the oxide scale formed frequently contains crystalline products, bubbles and shows cracks at the interface between the scale and the ceramic matrix. A model has been developed to account for the non-parabolic rate law behaviour. This model, which has been described in detail in Ref (1), is based on the assumption that the deviations from parabolic rate law behaviour can be attributed to a decrease of the cross section area, A , through which the rate controlling species diffuses.

Based on experimental observations concerning the devitrification of the amorphous scale and of the formation of bubbles and cracks, and assuming that the essential features of the parabolic rate law ought to be valid, a function, A(t) , describing the magnitude, $f*A_0$ with $0 \leq f \leq 1$, and rate, β, which A decreases with time has been derived and incorporated into the parabolic rate law (1). A new rate law is than obtained, which reads

$$\Delta W/A_o = a*\arctan\sqrt{bt} + c\sqrt{t} \qquad (2)$$

where a, b, and c are constants; and K_p in equation 1 can be evaluated from these constants according to

$$K_p = (a\sqrt{b} + c)^2 \qquad (3)$$

As mentioned above, parabolic rate law behaviour is rather frequently observed after a certain time t_0 of the experiment. Thus, for $t > t_0$

$$(\Delta W/A_o)^2 = K_p^o t + B_o \qquad (4)$$

where the apparent rate constant K_p^o is related to K_p in equation 1 through

$$f^2 K_p = K_p^o(t_o/(t_o+(B_o/K_p^o))) \qquad (5)$$

with f equal to the fraction of the initial area A_0 which still is amorphous at t_0. The value of f can be obtained from the relation

$$f = (a\sqrt{b}*(bt_o + 1)^{-1} + c)/(a\sqrt{b} + c) \qquad (6)$$

To the extent that β^{-1} is equal to t_0, the new rate law reads

$$\Delta W/A_o = a_1\sqrt{t} + b_1*t^{3/2} \qquad (7)$$

where a_1 and b_1 are equal to $\sqrt{K_p}$ and $-(1/3)a_1\beta(1-f)$, respectively.

In this article, the oxidation behaviour of different Si_3N_4-based ceramics is discussed within the framework of this new approach. Four oxidation curves of three different materials will thus be presented, and it will be shown that two of these curves can be fitted to equations 1 and 2, respectively. The other two oxidation curves obey equations 2 and 7, respectively, for $t < t_0$, while for $t \geq t_0$ equation 4 is shown to be applicable in both cases.

2. EXPERIMENTAL

The oxidation curves of Si_2N_2O obtained at 1300 and 1600 °C are given in Figures 1 and 3. The fully dense ceramic pieces used were prepared by HIP technique without any sintering aid. The oxidation curve of a β-sialon material of the composition $Si_{6-z}Al_zO_zN_{8-z}$ with $z = 3.5$, prepared by pressureless sintering technique using a sintering aid of YAG ($Y_3Al_5O_{12}$) composition, is given in Figure 2. Finally, the oxidation curve of an almost monophasic α-sialon ceramic is given in Figure 4. Fully dense ceramic pieces of the latter material were prepared by pressureless sintering technique using 6 wt% Y_2O_3 as sintering aid. Details concerning the preparation techniques applied, the X-ray characterizations and microstructures of Si_2N_2O, β- and α-sialon materials used are given in Refs. 1,2 and 3, respectively.

The oxidation experiments were performed in a TG unit (SETARAM TAG24), provided with two symmetrical furnaces; one used for the oxidation of the sample and the other for the inert reference. The resolution of the TG unit is better than 2μg and precise regulation of the gas flow (dry oxygen) over the specimens kept the drift of the baseline within $\mp$ 5 μg during a 20-hour experiment. Ceramic pieces of the approximate size 15x15x1 mm^3 were oxidized; prior to the oxidation these specimens had been carefully polished with diamond paste (grains down to a size < 1μm) and cleaned in an ultrasonic bath.

3. RESULTS AND DISCUSSION

The experimental and calculated weight gain and the squared weight gain curves of Si_2N_2O oxidized at 1300 °C are given in Figure 1. It is interesting to note that the experimental data can be fitted equally well by equation 1 and 2. The K_p and B values obtained from equation 1 and the a, b, c and K_p values obtained from equation 2 are given in Table 1. In this case f is very close to 1, because bt_0 in equation 6 must be << 1 as b $= 9.88x10^{-9}$ and t_0 is approximately equal to the time of the experiment ($\approx$ $7x10^4$ seconds). It can be shown that with f = 1 the arctan function transforms into the parabolic one and accordingly the K_p values obtained from the two equations ought to be very similar in agreement with the calculations.

The weight gain and squared weight gain curves of a β-sialon ceramic of the composition $Si_{6-z}Al_zO_zN_{8-z}$ with $z = 3.5$, oxidized at 1350 °C, are given in Figure 2. In this case the deviation from parabolic rate law behaviour is small, as the experimental data can fairly well be fitted by equation 1. However, the experimental data obey the arctan function much better. The later part of the squared weight gain curve can be fitted by equation 4 and the K_p^0 and B_0 values thus obtained can be used, together with the K_p value from equation 2, to calculate f and t_0 from equations 5 and 6. The resulting t_0 value exceeds the time of the experiment. This is interpreted to mean that the oxidation curve obeys the arctan function over the entire time of the experiment.

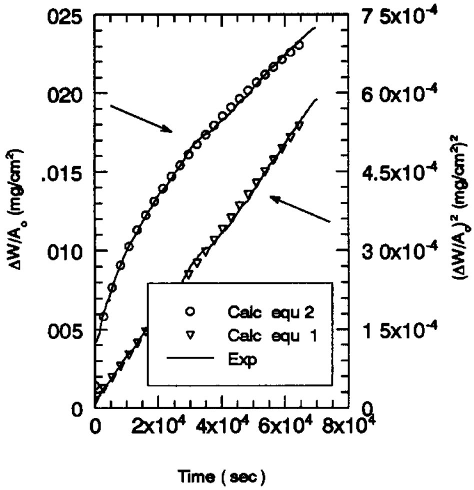

Figure 1. Experimental and calculated oxidation curves for Si_2N_2O at 1300 °C.

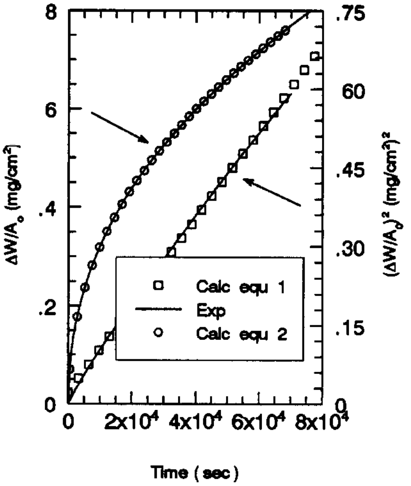

Figure 2. Experimental and calculated oxidation curves for a β-sialon ceramic (1350 °C).

The oxidation curves of Si_2N_2O obtained at 1600 °C are given in Figure 3. The later part of the squared weight gain curve can be fitted by equation 4, while the first part obeys the arctan function. The various constants obtained are given in Table 1. The f and t_0 values are obtained as above.

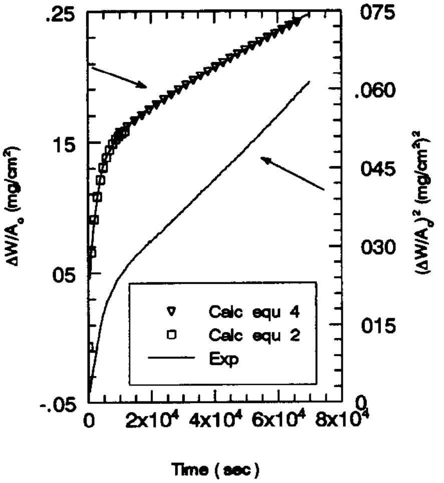

Figure 3. Experimental and calculated oxidation curves for Si_2N_2O at 1600 °C.

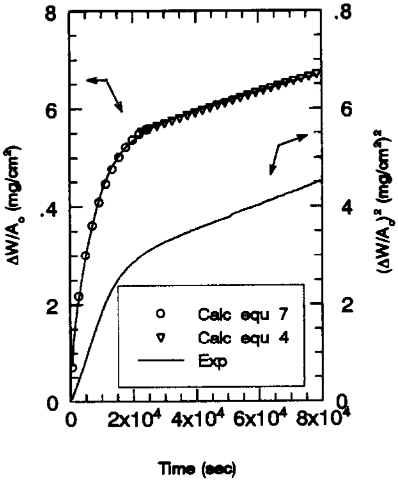

Figure 4. Experimental and calculated oxidation curves for an α-sialon ceramic (1350 °C).

Finally, the oxidation curves of the α-sialon ceramic at 1350 °C are given in figure 4. Again the later part of the squared weight gain curve can be fitted nicely by equation 4 while for $0 \le t \le 2\text{x}10^4$ equation 7 is obeyed. The obtained constants are given in table 1.

Table 1.
A tabular summary of the obtained constants in equations 1, 2, 4 and 7, and calculated K_p, K_p^o, f and t_o values for the oxidation curves of Si_3N_4-based ceramics.

Constants	Sample Si_2N_2O (1300)	 β-Sialon	 Si_2N_2O (1600)	 α-Sialon
$a/10^{-2}$ (mg cm^{-2})	85.8	7.52	71.1	
$b/10^{-4}$ (sec^{-1})	$9.88\text{x}10^{-5}$	1.42	0.451	
$c/10^{-4}$ (mg cm^{-2} s$^{-0.5}$)	0.0206	2.55	-26.6	
$a_1/10^{-3}$ (mg cm^{-2} s$^{-0.5}$)				5.38
$b_1/10^{-8}$ (sec$^{-1.5}$)				-6.02
$K_p/10^{-7}$ (mg^{2}cm^{-4}s^{-1})	0.081*	119	44.7	289
$K_p^o/10^{-7}$ (mg^{2}cm^{-4}s^{-1})			6.00	25.3
B_o (mg^2 cm^{-4})			0.019	0.252
f	1	0.76	0.19	0.33
t_o (sec)	-	∞	$1.2\text{x}10^4$	$2\text{x}10^4$

*A K_p value of $0.076\text{x}10^{-7}$ is obtained using equation 3.

In conclusion, it has been shown that the experimental oxidation curves of various Si_3N_4 based ceramics can satisfactory be interpreted with the parabolic rate law (equations 1 and 4) and/or the new rate laws (equations 2 and 7).

4. ACKNOWLEDGEMENT

This work has been finacially supported by the Swedish Board for Technical Developement.

5. REFERENCES

1. J. Persson, P.-O. Käll and M. Nygren, Submitted to J. Am. Ceram. Soc.
2. J. Persson, P.-O. Käll and M. Nygren, Submitted to J. Eur. Ceramics.
3. J. Persson, P.-O. Käll and M. Nygren, Proc. from Austceram 92, International Ceramic Conf., Melbourne, Australia 1992.